A System for Limb-Volume Measurement using 3D Models from an Infrared Depth Sensor

Guannan Lu[1], G. N. DeSouza[2], Jane Armer[3], Blake Anderson[4], and Chi-Ren Shyu[5]
ViGIR - Vision-Guided and Intelligent Robotics Lab, ECE Department[1,2]
Sinclair School of Nursing[3]
MU Informatics Institute[4,5]
University of Missouri
349 Eng. Building West, Columbia, MO, 65211
Email: [1]glfx3@mizzou.edu, [2]DeSouzaG@missouri.edu,
[3]Armer@missouri.edu, [4]AndersonBl@missouri.edu, [5]ShyuC@missouri.edu

***Abstract*—Lymphedema, a chronic disease caused by failure in the lymphatic system, affects nearly 500,000 people in the U.S., and over 2.4 million breast cancer survivors are at-risk for developing this disease at some point in their life. Early detection and management can significantly reduce the potential for symptoms and complications; however, many patients fail to seek medical assistance at the first sign of the disease. In this paper, we present a method for measuring limb volume and for detecting early swelling associated with lymphedema. The system relies on IR imaging sensors, such as in the Microsoft Kinect. This technique will allow for the future development of tools for self-management and specialist monitoring, and when compared to other commercially available devices, our system is less expensive, equally or more reliable/accurate, and much more user friendly.**

I. Introduction

Secondary lymphedema (LE) results from the disruption or obstruction of lymphatic pathways, which in the U.S. occurs most commonly as a result of cancer treatment, particularly in patients who require surgical removal of (or radiation to) lymph nodes. The result is reduced lymphatic flow with increased pressure in remaining lymphatic channels and accumulation of protein-rich fluid in the tissues. This process then initiates an inflammatory reaction leading to fibrosis, impaired immune responses, and fatty degeneration of connective tissue [1]. The underlying physiological, biological, and molecular mechanisms are not fully understood at this time. Lymphedema is often classified by stage, based on severity of the condition. The range of conditions may be latent (i.e. no swelling is present despite impaired lymph transport) to accumulation of fluid resulting in severe limb swelling (i.e. increase in limb volume of 40% or greater) [2]. Lymphedema may be debilitating and distressing even in early stages [3]. Physical impairments associated with LE include difficulty sleeping, carrying objects, exercising, and finding well-fitting clothing [4]. Additionally, LE patients report having lowered quality of life and a negative body image perception [5]. Due to the lack of a "gold standard" for LE diagnosis and measurement imprecision, the true occurrence of LE is unknown. Based on conservative figures of LE incidence [6], it is estimated that nearly 500,000 breast cancer survivors currently suffer from LE and it is projected that 2.4 million are at lifetime LE risk in the U.S. alone.

While LE is not a curable condition, it can be managed most successfully with early detection and initiation of appropriate therapy [7]. Despite the importance of early intervention, many patients and health care providers are unaware of the early signs and symptoms associated with LE. Increasing the frequency of visits to a specialist would increase the potential for detecting LE in its early stages, however, with the abundance of Internet technologies, mobile devices, and the potential to collect and share data on a large scale, it is likely that patients and therapists can more effectively monitor risks and symptoms without the need for more frequent appointments.

Currently, when a patient visits their specialist, volume measurements are performed through the water displacement, circumference, impedance, perometry, or the DEXA scan methods (summarized in Table I), which have been extensively compared in the literature [8], [9]. Water displacement is the 'gold standard' measure of volume where the amount of displaced water represents the volume of the submerged limb [10]. However, the patient must remain still, the vertical orientation of the limb makes this method difficult to replicate with other methods, and the cleanup and disinfecting process is burdensome. Circumference measures can be taken with a tape at specific points along the limb and the total volume can be estimated by assuming cylindrical or conic volumes between the points. However, this method requires careful identification of consistent anatomical regions for reliability across measures [11]. Impedance involves attaching electrodes at points along the limb and measuring the electrical signals [12]. This method has a high lifetime operational cost due to disposable electrode attachments. On the other hand, the perometry uses infrared to scan along the limb and assess circumferences at 0.5cm intervals [13]. This method has become popular, but is cost-prohibitive for many settings. Finally, there is the DEXA Scan, or Dual Energy X-ray Absorptiometry, which was typically used to measure bone density and has been successfully employed for soft tissue. Its high-end, 6-figure cost makes it definitely not appropriate for self monitoring.

Table I
EVALUATION MATRIX OF EXISTING METHODS AND THE THE PROPOSED METHOD FOR VOLUME MEASUREMENT

	Displacement	Circumference	Impedance	Perometry	DEXA Scan	Proposed Method
Cost	Low	Low	High	High	High	Low
Time to Operate	Low	High	Low	Low	Low	Low
Inter-Rater Disparity	Low	High	Low	Low	Low	Low
Pre and Post Maintenance	High	Low	High	High	High	Low
Local Measures	No	Yes	No	Yes	Yes	Yes
Self-monitoring Home/Travel	No	Yes	No[1]	No	No	Yes

[1] *Impedimed* is exploring market for home use of their device

Technologies for 3D reconstruction for human bodies and other objects have been around for many years [14], [15], [16], [17], [18], [19], [20], [21]. They provide very accurate and reliable models, which can be used for measuring limb volumes with equal or better accuracy than the methods used today. Besides, they can be much more user-friendly and allow for self-monitoring.

In this paper, we proposed a method that can be utilized at home or clinic, and it can be easily operated by professionals and non-professionals without any special training. Our method only requires an IR sensor, such as the Microsoft Kinect, which is used to capture multiple views of the human arm. The method relies on the Iterative Closest Points (ICP) algorithm [16] to compute the registration between two adjacent views.

The proposed volume-measurement method takes just a couple of minutes to acquire the images. It has low cost, high accuracy and low cleanup. It is also capable of capturing local swelling sites (an indicative symptom of the early stages of lymphedema). Further, because patients can perform the measurements at home, those measurements can be taken at much more frequent intervals. Figure 1 depicts the typical setup for the perometry scan and the proposed method, which will be later compared in this paper.

The paper is organized as follows: first, a background on sensor calibration is provided in section II. Next, the proposed method is explained in section III. Then, the experimental results are provided in section IV. Finally, the conclusions and future work are stated in section V.

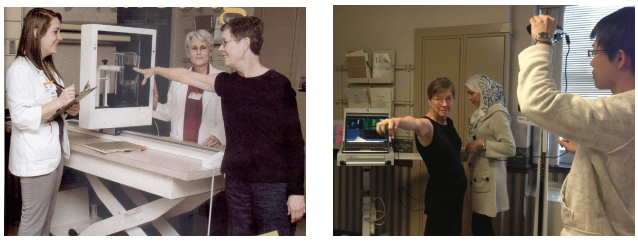

Figure 1. Setup for limb-volume measurement using the Perometry scanner (left) and the proposed IR scanner (right).

II. BACKGROUND

A. Background of Human Body 3D modeling

Technologies for 3D reconstruction of human bodies have been around for many years. In fashion and gaming industry, for example, human body modeling can be a very lucrative tool. More recently, 3D modeling of the human body has been suggested for many applications in medicine and health care, such as for dermatology [18], rehabilitation [22], [23], assisted living [24], etc..

Despite being a topic currently in high demand, 3D modeling of the human body poses a great challenge, especially in health care, due to the human body being a non-rigid object and the human skin having few features that can be used by registration algorithms. In that sense, while earlier approaches employing multi-view stereopsis [17], [18], [19], [20] could build 3D models from simple 2D images, they were also not as reliable as newer methods based on new IR sensing technologies. Besides, they required well calibrated cameras [17], [18] and some times, a setup of multiple cameras [19], [20]. In the work presented in [15], human bodies were modeled using laser scanners. The method allowed for the modeling of a large number of human bodies (250) and it provided very accurate models, but it also required an expensive device for range imaging (over US$20,000) and it was quite difficult to be handled by non-professionals.

On the other hand, new technologies relying on IR imaging are becoming more pervasive in health care and rehabilitation, mainly because they do not force the human subject to be still throughout the image acquisition process. A recent method presented in [14], also relying on inexpensive IR sensors, produced models with less than 6cm of error, in less than 4 seconds. However, templates of the human body needed to be created before any modeling could be done. In that system, building even a rough template of the human body can represent a complicated and tedious task. Besides, a setup with multiple IR sensors had to be created around the human subject, which makes the process inadequate for self-monitoring applications.

In another recent paper, the SCAPE (Shape Completion and

Animation of PEople) approach was proposed [25]. The paper introduces a new and effective approach using silhouettes and depth data from one single IR sensor. However, the main disadvantage of the system is that a detailed shape can take 65 minutes to be optimized.

In this paper, we propose a method that can be operated by professionals as well as non-professionals in the comfort of their clinics or homes. Our method requires only one IR sensor. The sensor is used to capture different views of the human subject while its moved around that subject. The views are combined by the ICP algorithm [16], which processes the images and computes their registrations. Finally, a Poisson surface reconstruction method ([26]) is applied to generate the final 3D model.

III. Proposed System

Our method consists of five major steps. The framework is shown in Figure 2 and the steps are: 1) Raw Image Capture; 2) Coarse Registration; 3) Fine Registration; 4) Common Reference Registration; and 5) Filtering and Surface Reconstruction.

In the next subsections we will detail each of those steps.

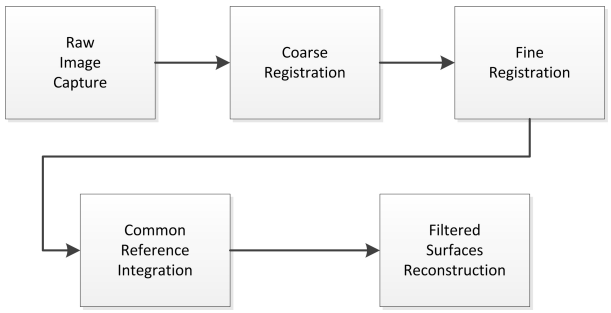

Figure 2. Block diagram with the steps of our framework

A. Image Capture

Our system employs a commercially available and quite inexpensive IR sensor: the Microsoft Kinect. Despite the relative low resolution offered by this device, 640x480, it allows us to collect images very quickly, at 30fps. So, we opted for acquiring a large number of low-resolution images and increase the accuracy of the final model by the registration of multiple, redundant images.

The only constraint imposed by this step is for the user to hold the device at a distance of approximately 80cm to the target limb. At that distance, the device provides the most accurate depth detection. The user can then freely move the device around the subject while keeping the same approximate distance of 80cm to the subject. The output of the device is a raw depth image, which is calibrated into actual world coordinates using the algorithm in [27]. The result is illustrated in Figure 3.

B. Coarse and Fine Registrations

The next two steps of the proposed framework is the Coarse and Fine Registrations. The goal of both of these steps is to register pairs of consecutive depth images into the same 3D coordinate frame, and iteratively to register all pairs into a single 3D reference coordinate frame [21]. The process starts with a graphical user interface that allows for an easy initialization of the registration process – i.e. the coarse registration. A snapshot of the GUI is presented in Figure 4. The GUI allows the user to click on a set of four corresponding points on two consecutive images. These points are then used by the coarse registration, and the result of the coarse registration is automatically fed into the fine registration, leading to a complete set of points with respect to the same reference frame.

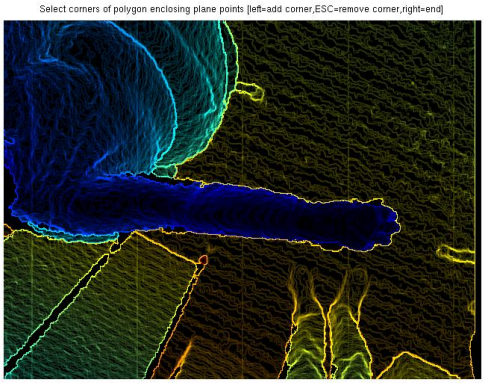

Figure 3. Sample depth-image of an arm obtained by our method.

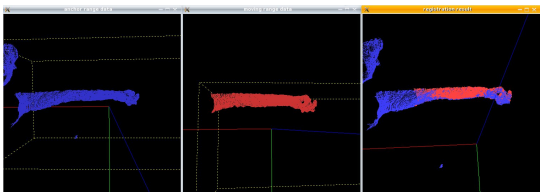

(a) (b) (c)

Figure 4. Graphical User Interface used for registration: (a) current depth image; (b) previous depth image; (c) registered images.

In the future, we will replace the coarse registration process by an automated method involving gyroscopes and accelerometers attached to the IR device. These motion sensors will provide all the information necessary to initiate the fine registration process and eliminate any human interaction from the loop.

The fine registration is accomplished by the ICP algorithm [16]. As we mentioned earlier, the fast frame rate obtained by the use of the IR device guarantees that two consecutive views always present overlapping regions. This fact allows the ICP algorithm to provide a very robust registration of the two clouds of points. The output of the ICP algorithm is a homogeneous transformation matrix containing the rotational and translational components relating a pair of consecutive

views. Our framework then iteratively transforms all the pairs of views to the same reference frame. That is, as the framework process the pair i and $i-1$, it calculates the homogeneous matrix:

$$^{i}H_{r} = {}^{i}H_{i-1} * {}^{i-1}H_{r}$$

where i represents the index of the current view, $i-1$ is the previous view, $^{i}H_{i-1}$ is the homogeneous matrix computed by ICP algorithm, and $^{i-1}H_{r}$ is the transformation – with respect to the reference frame r – of all views up to that point in the iteration of the framework.

C. Common Frame Integration

As we mentioned above, our approach to achieve high-density models was through the use of multiple and redundant depth images. This process leads to a set of depth images with great overlaps between them. This property is at the same time desirable and a burden to the system: while it provides a dense and accurate model of the arm, it also leads to large datasets. In this step of the framework, we must eliminate any redundancy in the dataset. Currently, this is achieved by a simple elimination of redundant depth images from the dataset. An integration algorithm discussed in [21] will replace this step in the future.

D. Filtering and Surface Reconstruction

The last step in the framework consists of filtering and surface reconstruction. In order to achieve a smooth surface reconstruction our framework performs several substeps. First, in order to reduce the computation complexity, the point clouds are sub-sampled. Next, Poisson-disk sampling is processed on the point clouds. For this application involving the human arm, we noticed that a total of 10000 points is enough for good reconstruction. Since the computation of the normals on the surface of the object is required for the final substep, our framework estimates the normals using 10 neighboring points. Finally, the Poisson algorithm [26] for surface reconstruction is employed using an octree depth of 12, a solver divide of 8, a number of samples per node equal to 3 and a surface offsetting of 1.

The final result of this surface reconstruction and all the previous steps is presented in the next section.

IV. Experimental Results and Discussion

In order to evaluate the accuracy and usefulness of our method for the target application of limb-volume measurement, we performed two different experiments. In the first experiment, we compared our method against the perometry method. In the second experiment, we focused on the the accuracy and ability of the proposed method to detect localized swells.

It is important to mention here that the perometry method cannot be considered as ground truth, since its application in lymphedema is predicated upon its ability to provide repeatability, but not necessarily accuracy in the readings. Our goal in comparing with the perometry method was simply to use it as a basis for the comparison of this same repeatability.

A. First Experiment

For this experiment, we collected data for a total of twelve arms, from six different human subjects. Also, five of those individuals were healthy people, while the last one was from a person with lymphedema. Here, we present the volume for the three most typical cases and for the case of lymphedema.

Both the perometer and our method require the user to manually select the region to be measured – i.e. the length of the arm for which the volume must be calculated. Since this is part of the protocol employed by clinicians, in both cases we manually removed the image of the hand and the upper parts of the arm. The calculated volumes obtained by the two devices are listed at the end of this section, in Table II.

For a qualitative analysis of the results obtained by our method, we present the result of all four experiments reported here in the next four figures.

In Figure 5, we present the first of these experiments. This model was constructed using 20 views. It may be difficult for the reader to see without zooming into the figure, but the number on the right side of the arm is the length of that arm – in this case, $474mm$. That same length reported by the perometer was $470mm$.

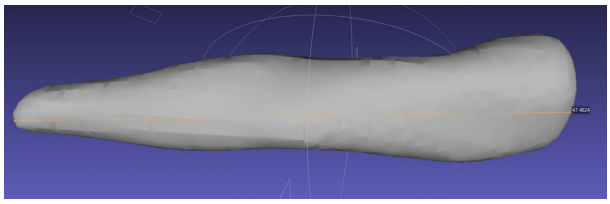

Figure 5. 3D model of the first human subject

The second model was built using 25 views. Once again, the number on the right side of the arm, which can be read by zooming into the picture, represents its length as reported by our method and is equal to $481mm$. The length of the arm from the perometry device was $480mm$. Figure 6 depicts the model obtained for this subject.

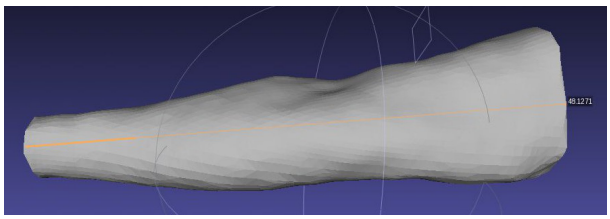

Figure 6. 3D model of the second human subject

The third test model, presented in Figure 7, was built using 19 views. The length of the arm as reported by our method

was $364mm$, and the length reported by the perometer was $376mm$. This was the largest discrepancy observed by this comparison between our method and the perometry and it can be attributed to the fact that the arm in Figure 7 does not appear to be completely stretched.

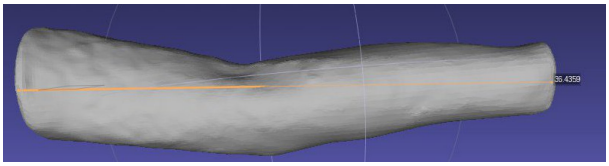

Figure 7. 3D model of the third human subject

Finally, the fourth test model was built using 18 views. This model was created by imaging the arm of a person with lymphedema, as it can be observed in Figure 8. The number on the right side of the arm, which again indicates its length, is $364mm$. The length of the model reported by the perometer was $372mm$.

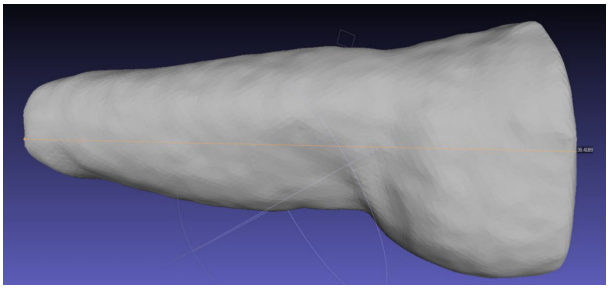

Figure 8. 3D model of the human subject with lymphedema

Once again, in Table II we compare the volumes obtained with our method and the perometry device. The percentage discrepancy in the third column of the table was calculated by dividing the volume difference between the two measurements and the volume from our method.

The results obtained by the proposed method have a percentage discrepancy of less than 13% with respect to the perometry. This shows the robustness of our method. Since the most important property of any method for lymphedema detection is *intra-rater* reliability/repeatability – i.e. the ability of the method to detect change from baseline over time – the perometry method should be seen as *ground truth*. In fact, in perometry it is acceptable a change of no more than $\pm 50ml$ in a volume of about $2400ml$.

Another important point to be made is regarding the selection of the extents of the arms used for volume calculation. Since for both devices this selection was done manually, it is possible that despite similar lengths were observed, slight shifted extents of the arms were used. This shift could explain the difference in volumes also observed in Table II. In the future a consistent procedure to select the arm extents must be imposed between both methods.

In order to address the more typical *engineering* criteria against ground truth, we performed another experiment using an object of known volume.

B. Second Experiment

This experiment was conducted with two main objectives: 1) to show that the proposed method is able to detect small and localized swelling of the arms; and 2) to determine the resolution of this measurement. For that, we taped a small pen to the arm of a human subject. Figure 9 shows the 3D model obtained for this experiment. The shape and volume of the pen were then estimated from the same 3D model and the value of $9.2ml$ was calculated for the volume. This is a great achievement considering the ability of the proposed system to detect swellings as small as 0.5% of the volume of the arm. However, the real volume of the pen was estimated to have a volume of $11.6ml$ – i.e. an error of 20% with respect to the ground truth. Given that the error of the instrument used, the Kinect, is more than $1cm$ – i.e. the calibration method used does not provide accuracy better than $1cm$ ([27]) – it is reasonable to expect large percentage errors in such small volumes.

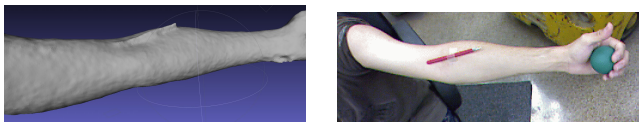

(a) (b)

Figure 9. Test of the detection of localized swelling.

V. Conclusion and Future Work

We proposed a new and convenient system to accurately model the human arm. As the experimental results demonstrated, our method is robust and it presents the ability to detect small and localized differences in limb volume. This method relies on an IR device that is much smaller and inexpensive than the emerging research and commercial standard: the perometry. Besides, it can be operated by any person, with no training and in the convenience of their homes or clinics. Our method shows a significant advantage over other commercial devices, including price, ease of use, and maintenance.

In the future, we will improve the coarse registration, by employing gyroscopes and accelerometers to detect the motion of the device and to automate the registration process. Also, a more elaborate integration algorithm will allow us to keep a larger number of views and at the same time reduce the size of the data set by eliminating redundant points. Analysis of the effects of the distance between the device and the arm on the accuracy of the measurements should also be carried out. Finally, we intend to compare our method using the same methodology as the one described in [[8], [9]] as well as using

Table II
VOLUME AND LENGTH COMPASSION

Test	Proposed method (Volume in ml)	Perometry device (Volume in ml)	Percentage Discrepancy	Proposed method (Length in mm)	Perometry device (Length in mm)	Percentage Discrepancy
1	1972	1878	4.7	474	470	0.8
2	3581	3122	12.8	481	480	0.2
3	1570	1381	12.0	364	376	3.3
4	3756	3393	9.6	364	372	2.2

the water displacement method. In summary, more quantitative measurements should provide final evidence of the increased applicability and reliability of our method over other options, in especial the water displacement, which is still regarded as the golden standard in the field.

REFERENCES

[1] P. Mortimer, "Chronic peripheral oedema: the critical role of the lymphatic system." *Clinical Medicine*, vol. 4(5), pp. 448–453, 2004.

[2] International Society of Lymphology, "The diagnosis and treatment of peripheral lymphedema: consensus document of the international society of lymphology," *Lymphology*, vol. 36, p. 9, 2003.

[3] J. M. Armer, M. E. Radina, D. Porock, and S. D. Culbertson, "Predicting breast cancer-related lymphedema using self-reported symptoms," *Nurs Res*, vol. 52(6), pp. 370–09, 2003.

[4] M. M. Hull, "Functional and psychosocial aspects of lymphedema in women treated for breast cancer," *Innovations in Breast Cancer Care*, vol. 3(4), pp. 97–100, 1998.

[5] G. Jager, "Quality-of-life and body image impairments in patients with lymphedema," *Lymphology*, vol. 39, pp. 193–200, 2006.

[6] J. A. Petrek and M. C. Heelan, "Incidence of breast carcinoma-related lymphedema," *Cancer*, vol. 83(12 Suppl American), pp. 2774–2781, 1998.

[7] E. G. Poage, "Lymphedema: What interventions are effective in reducing risk for and treating secondary lymphedema?" *Oncology Nursing Society*, 2008.

[8] S. H. Ridner, L. D. Montgomery, J. T. Hepworth, B. R. Stewart, and J. M. Armer, "Comparison of upper limb volume measurement techniques and arm symptoms between healthy volunteers and individuals with known lymphedema," *Lymphology*, vol. 40, no. 1, pp. 35–46, March 2007.

[9] J. M. Armer and B. R. Stewart, "A comparison of four diagnostic criteria for lymphedema in a post-breast cancer population," *Lymphatic Research and Biology*, vol. 3, no. 4, pp. 208–217, 2005.

[10] A. Sagen, R. Karesen, P. Skaane, and M. A. Risberg, "Validity for the simplified water displacement instrument to measure arm lymphedema as a result of breast cancer surgery," *Arch Phys Med Rehabil*, vol. 90, pp. 803–809, May 2009.

[11] R. Taylor, U. W. Jayasinghe, L. Koelmeyer, O. Ung, and J. Boyages, "Reliability and validity of arm volume measurements for assessment of lymphedema," *Phys Ther*, vol. 86, pp. 205–214, Feb 2006.

[12] A. G. Warren, B. A. Janz, S. A. Slavin, and L. J. Borud, "The use of bioimpedance analysis to evaluate lymphedema," *Annals of Plastic Surgery*, vol. 58, no. 5, 2007.

[13] A. W. Stanton, J. W. Northfield, B. Holroyd, P. S. Mortimer, and J. R. Levick, "Validation of an optoelectronic limb volumeter (perometer)," *Lymphology*, vol. 30, no. 77, 1997.

[14] J. Tong, J. Zhou, L. Liu, Z. Pan, and H. Yan, "Scanning 3d full human bodies using kinects," *IEEE Transactions on Visualization and Computer Graphics*, vol. 18, no. 4, pp. 643–650, april 2012.

[15] B. Allen, B. Curless, and Z. Popovic, "The space of human body shapes: reconstruction and parameterization from range scans." *ACM Transactions on Graphics*, vol. 22, no. 3, pp. 587–594, 2003.

[16] P. J. Besl and N. D. McKay, "A method for registration of 3D shapes," *IEEE Transactions on Pattern Analysis and Machine Intelligence*, vol. 14, no. 2, pp. 239–256, February 1992.

[17] D. Lam, R. Hong, and G. N. DeSouza , "3D human modeling using virtual multi-view stereopsis and motion estimation," in *Proceedings of the 2009 IEEE International Conference on Intelligent Robots and Systems*, Oct. 2009, pp. 4294–4299.

[18] D. Lam and G. N. DeSouza , "Virtual dermatologist: An application of 3D modeling to tele-healthcare," in *Proceedings of the 13th IEEE International Conference on e-Health Networking, Application & Services*, June 2011, pp. 28–33, columbia, MO (Selected for Best Paper Award).

[19] Y. Furukawa and J. Ponce, "Accurate, dense and robust multi-view stereopsis," in *Proceedings of IEEE International Conference on Computer Vision and Pattern Recognition*, 2007, pp. 1–8.

[20] ——, "Accurate, dense, and robust multiview stereopsis," *Pattern Analysis and Machine Intelligence, IEEE Transactions on*, vol. 32, no. 8, pp. 1362–1376, Aug. 2010.

[21] J. Park and G. N. DeSouza, *3-D Modeling of Real-World Objects Using Range and Intensity Images.*, ser. Studies in Computational Intelligence, B. Apolloni, A. Ghosh, F. N. Alpaslan, L. C. Jain, and S. Patnaik, Eds. Springer-Verlag, 2005, vol. 7. [Online]. Available: http://dblp.uni-trier.de/db/series/sci/sci7.html#ParkD05

[22] B. Lange, C.-Y. Chang, E. Suma, B. Newman, A. Rizzo, and M. Bolas, "Development and evaluation of low cost game-based balance rehabilitation tool using the microsoft kinect sensor," in *Engineering in Medicine and Biology Society,EMBC, 2011 Annual International Conference of the IEEE*, 30 2011-sept. 3 2011, pp. 1831–1834.

[23] I. Pastor, H. Hayes, and S. Bamberg, "A feasibility study of an upper limb rehabilitation system using kinect and computer games," in *Engineering in Medicine and Biology Society (EMBC), 2012 Annual International Conference of the IEEE*, 28 2012-sept. 1 2012, pp. 1286–1289.

[24] B. Jansen, F. Temmermans, and R. Deklerck, "3d human pose recognition for home monitoring of elderly," in *Engineering in Medicine and Biology Society, 2007. EMBS 2007. 29th Annual International Conference of the IEEE*, aug. 2007, pp. 4049–4051.

[25] D. Anguelov, P. Srinivasan, D. Koller, S. Thrun, J. Rodgers, and J. Davis, "Scape: shape completion and animation of people," *ACM Trans. Graph.*, vol. 24, no. 3, pp. 408–416, Jul. 2005. [Online]. Available: http://doi.acm.org/10.1145/1073204.1073207

[26] M. Kazhdan, M. Bolitho, and H. Hoppe, "Poisson surface reconstruction," in *Proceedings of the fourth Eurographics symposium on Geometry processing*, ser. SGP '06. Aire-la-Ville, Switzerland, Switzerland: Eurographics Association, 2006, pp. 61–70. [Online]. Available: http://dl.acm.org/citation.cfm?id=1281957.1281965

[27] D. Herrera C., J. Kannala, and J. Heikkil, "Joint depth and color camera calibration with distortion correction," *Pattern Analysis and Machine Intelligence*, vol. 34, no. 10, pp. 2059–2064, 2012.